JOURNAL OF Materials CHEMISTRY

Z-Isomers of 3,3′-disubstituted azobenzenes highly compatible with liquid crystals

Christian Ruslim and Kunihiro Ichimura*

Research Laboratory of Resources Utilization, Tokyo Institute of Technology, 4259 Nagatsuta, Midori-ku, Yokohama 226, Japan. E-mail: kichimur@res.titech.ac.jp

Received 19th October 1998, Accepted 4th December 1998

It is known that mesophase changes can be induced by *E–Z* photoisomerization of azobenzenes doped in liquid crystals. Novel azobenzenes have been designed on the basis of Molecular Mechanics and Molecular Orbital calculation, aimed at exploiting novel photoresponsive guest–host liquid crystalline systems exhibiting no mesophase change despite the drastic structural alteration of the guest molecules. It was found that the introduction of alkanoyloxy groups at both the 3- and 3′-positions of azobenzene leads to phase stability of nematic systems upon the *E–Z* photoisomerization even at a dopant concentration as high as 20 wt%. However phase separation was brought about when 3,3′-dialkoxyazobenzenes and 4,4′-dialkoxyazobenzenes were employed as guest molecules. The relation between the conformational structures of the guests in their *E*- and *Z*-isomers and their compatibility with nematic hosts was examined thermodynamically. Experimental results were compared in some details with the simulations. It was shown that 3,3′-dialkanoyloxyazobenzene prefers a *rod-like* structure in both *E*- and *Z*-isomers.

The modification of mesophases with light has attracted increasing attention because of providing access to a wide variety of areas such as optical switching, holography and optical information storage systems.[1–3] Photoresponsiveness in liquid crystal (LC) systems can be achieved by the manipulation of photoreactive guest molecules, or, in some cases, the liquid crystalline matrices themselves are photoreactive. Generally, azobenzenes or stilbenes undergo *E–Z* isomerization upon UV light irradiation. This process is reversible through photoirradiation or heat exposure. The photoisomerization is accompanied by prominent changes in the properties of the guest molecules and consequently of the surrounding mesophasic matrices so that the photochemistry leads to the emergence of photo-optical effects in the systems.[4] The geometrical photoisomerization of stilbenes[5] and azobenzenes[6] dissolved in nematic LCs leads to the disordering of the LC phase because of the predominant formation of *Z*-isomers with bent structures. This is the principle for the isothermal photochemical phase transition which has been proposed with a view to application in optical information storage.[2] Another exploitation of these photoisomerization characteristics was demonstrated by Sackmann[7] who reported the reversible change of the helical pitch of an azobenzene–cholesteric liquid crystal system upon photoisomerization. Heppke *et al.* introduced chiral *para*- and *ortho*-substituted azobenzenes in a nematic LC and investigated the molecular twisting power of the system which, in some cases, showed a reversible inversion of the helical sense on isomerization.[8] Hermann *et al.* reported the photoinduced change of flexoelectric anisotropy as a result of *E–Z* configurational change of an azobenzene dopant in a nematic liquid crystal and hence of the distribution of the dipole moment in the system.[9] In this novel photoresponsive LC system, a mesophase change needs to be avoided, in sharp contrast to cases based on the structural modification of photoresponsive guests directed towards isothermal photochemical phase transition. In other words, the mesophase has to be preserved in this case both before and after the photoisomerization of guests such as azobenzenes.

In this work, we report the effect of photoisomerization of guest 3,3′-disubstituted azobenzenes **1**–**4** on the stability of liquid crystalline hosts. Our interest is to design and develop photoresponsive liquid crystalline systems that exhibit phase

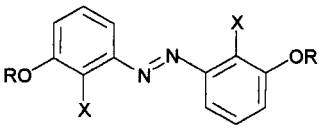

1: R = C_6H_{13}, X = H
2: R = C_6H_{13}, X = CH_3
3a: R = COC_3H_7, X = H
3b: R = COC_5H_{11}, X = H
3c: R = $COC_{11}H_{23}$, X = H
4: R = COC_5H_{11}, X = CH_3

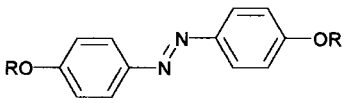

5: R = C_6H_{13}
6: R = COC_5H_{11}

stability upon photoisomerization. Our motivation in selecting 3,3′-disubstitution was the anticipation that an appropriate choice of substituents would give rise to the preferential formation of conformers in both *E*- and *Z*-isomers in which the terminal chains are stretched out to make the molecule rod-shaped. Accordingly, without disorganizing or destroying the liquid crystalline phase, changes in the guest molecular structure, *i.e.* changes in the properties of the guest or the entire system, can be manipulated so that they can be magnified by high concentration doping. Although some studies of the effect of molecular structures of azobenzenes on the nematic phase have been made,[10] all the compounds used have been 4-substituted or 4,4′-disubstituted such as **5** and **6**. Furthermore, there has been no report on the effect of 3,3′-disubstitution on the *E–Z* photoisomerization. To our knowledge, there are few detailed studies emphasizing conformational changes of photoresponsive molecules upon irradiation with light with respect to the stability of the liquid crystalline phase.

The effect of the *E–Z* photoisomerization of azobenzene dopants at high concentrations on a nematic phase is reported first. Then, the guest–host interaction is discussed through the

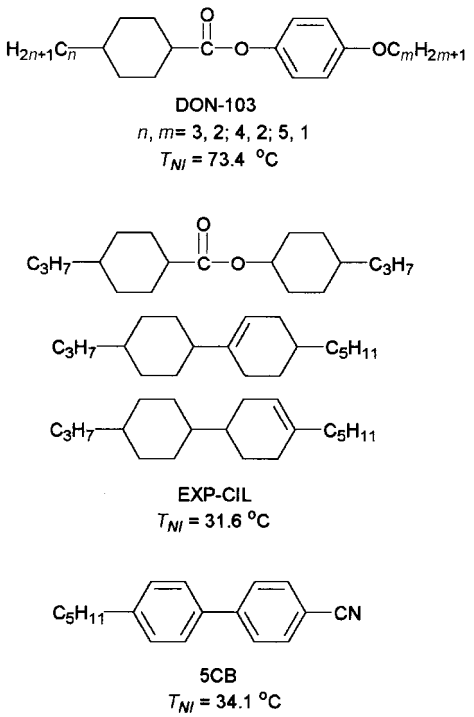

Fig. 1 Structures of nematic liquid crystal hosts and their phase transition temperatures.

nematic–isotropic phase equilibria. The correlation of the results with the photoinduced structural change of guest azobenzenes is evaluated, together with the calculated stable conformations provided by Molecular Mechanics and Molecular Orbital calculation. The chemical formula and the nematic–isotropic phase transition temperature T_{NI} of the host liquid crystals used in this experiment are shown in Fig. 1.

Experimental

Synthesis and characterization of materials

m-Nitrophenol, *p*-nitrophenol, 3,4-dihydro-2*H*-pyran, pyridinium toluene-*p*-sulfonate, 1-bromobutane and 1-bromohexane were purchased from Tokyo Chemical Industry. Butanoyl chloride, hexanoyl chloride and dodecanoyl chloride were purchased from Kanto Chemical and 2-methyl-3-nitrophenol was from Sigma Chemical. All reagents were used without further purification. Diethyl ether and THF were distilled over lithium aluminum hydride ($LiAlH_4$), DMF over molecular sieves, and dichloromethane over phosphorus pentaoxide. All solvents were stored over 4 Å molecular sieves.

The chemical structures of intermediates and final products were characterized by ^1H and ^{13}C NMR spectra, recorded on a Bruker AC-200 NMR Spectrometer with TMS as an internal standard (*J* values are given in Hz), and elemental analysis. Melting points were determined on a Yanaco MP-S3 micro melting apparatus, and phase transition temperatures of the final products were determined on a DSC 22C (Seiko Densi Kogyo) and a Polarizing Optical Microscope Olympus BH-2 equipped with a Mettler FP800 hot stage.

3-(2-Tetrahydropyranyloxy)nitrobenzene

m-Nitrophenol (14.5 g, 104 mmol) was dissolved in 45 mL CH_2Cl_2. To this solution were added 3,4-dihydro-2*H*-pyran (10 g, 119 mmol) and pyridinium toluene-*p*-sulfonate (2.8 g, 11 mmol). The mixture was stirred at 0 °C for 30 min and then for 2 h at room temperature. The mixture was washed several times with 3 mol dm^{-3} NaOH solution and distilled water, respectively, and dried over $MgSO_4$. After removal of the solvent and excess dihydropyran, the product was obtained as a brown oil. ^1H NMR ($CDCl_3$): δ(ppm) 1.68–2.08 (m, 6 H), 3.60–3.95 (m, 2 H), 5.50 (m, 1 H), 7.29–7.90 (m, 4 H).

3,3′-Bis(tetrahydropyran-2-yloxy)azobenzene

This was prepared according to the literature.[11] To a 1 L three-necked flask equipped with a thermometer, a mechanical stirrer and a dropping funnel were added dry ether (350 mL) and 4.4 g (116 mmol) of $LiAlH_4$. The solution was kept at −70 °C by using an ethanol–dry ice bath and stirred, while 3-(tetrahydropyran-2-yloxy)nitrobenzene, diluted with dry ether, was slowly added through a dropping funnel. After turning to a dark-brown suspension, the reaction was allowed to warm to room temperature gradually. After the disappearance of the reactant, monitored by TLC, the product was extracted with ether, and the organic phase was washed with distilled water, dried over $MgSO_4$, concentrated and dried *in vacuo* to give 11.4 g of product (58% from *m*-nitrophenol) as a dark orange powder (mp 96–98 °C). ^1H NMR ($CDCl_3$): δ(ppm) 1.65–1.91 (m, 12 H), 3.61–3.94 (m, 4 H), 5.54 (m, 2 H), 7.14–7.60 (m, 8 H). ^{13}C NMR ($CDCl_3$): δ(ppm) 18.7, 25.2, 30.4, 62.1, 96.4, 109.6, 117.5, 119.4, 129.7, 153.8, 157.8.

3,3′-Dihydroxyazobenzene

A solution of 3,3′-bis(tetrahydropyran-2-yloxy)azobenzene (11.4 g, 30 mmol) in methanol (150 mL) was refluxed with an excess of 2% aqueous oxalic acid for 1 h, and then extracted with ether. The product was purified through flash chromatography (silica gel, ethyl acetate–hexane (1 : 1)) and recrystallized from methanol to give 2.2 g (19% from *m*-nitrophenol) of product as a yellow powder (mp 211–213 °C). ^1H NMR (DMSO-d_6): δ(ppm) 6.94–7.40 (m, 8 H), 9.84 (s, 2 H). ^{13}C NMR (DMSO-d_6): δ(ppm) 107.1, 115.3, 118.6, 130.2, 153.2, 158.2. IR (KBr, cm^{-1}): 3290. Found: C, 67.71; H, 4.83; N, 12.75. Calc. for $C_{12}H_{10}N_2O_2$: C, 67.30; H, 4.67; N, 13.08%.

3,3′-Bis(hexyloxy)azobenzene 1

This was prepared from 3,3′-dihydroxyazobenzene (0.32 g, 1.5 mmol), 1-bromohexane (0.60 g, 3.6 mmol) and K_2CO_3 (0.62 g, 4.5 mmol) by means of the Williamson reaction in DMF (10 mL) at 75 °C. The product was purified through column chromatography (silica gel, ethyl acetate–hexane (1 : 3)) to give 0.43 g of **1** as a brownish orange solid (yield: 76%). ^1H NMR ($CDCl_3$): δ(ppm) 0.92 (t, J=6.8, 6H), 1.35–1.50 (m, 12H), 1.82 (quintet, J=7.8, 4 H), 4.05 (t, J= 6.6, 4 H), 7.01–7.55 (m, 8 H). ^{13}C NMR ($CDCl_3$): δ(ppm) 14.1, 22.6, 25.8, 29.2, 31.6, 68.3, 106.5, 117.0, 118.3, 129.7, 153.9, 159.9. Found: C, 75.62; H, 8.88; N, 7.24. Calc. for $C_{24}H_{34}N_2O_2$: C, 75.39; H, 8.90; N, 7.33%.

3,3′-Bis(butanoyloxy)azobenzene 3a

The esterification of 3,3′-dihydroxyazobenzene (0.43 g, 2.0 mmol) with butanoyl chloride (0.53 g, 5.0 mmol) in the presence of triethylamine (0.61 g, 6.0 mmol) was carried out in diethyl ether. A conventional work-up gave an orange solid which was then purified by recrystallization from ethyl acetate to produce 0.58 g of **3a** (yield: 82%). ^1H NMR ($CDCl_3$): δ(ppm) 1.07 (t, J=7.2, 6 H), 1.76–1.88 (m, 4 H), 2.58 (t, J= 7.4, 4 H), 7.20–7.66 (m, 8 H). ^{13}C NMR ($CDCl_3$): δ(ppm) 13.68, 18.47, 36.26, 114.96, 121.79, 124.33, 129.77, 151.45, 153.42, 171.90. Found: C, 67.66; H, 6.11; N, 7.86. Calc. for $C_{20}H_{22}N_2O_4$: C, 67.77; H, 6.27; N, 7.91%.

3,3′-Bis(hexanoyloxy)azobenzene 3b

This was prepared in the same way in 85% yield. ^1H NMR ($CDCl_3$): δ(ppm) 0.94 (t, J=6.6, 6H), 1.38–1.86 (m, 12 H), 2.59 (t, J=7.2, 4 H), 7.19–7.56 (m, 8 H). ^{13}C NMR ($CDCl_3$):

δ(ppm) 13.9, 22.3, 24.6, 31.3, 34.4, 115.0, 121.8, 124.3, 129.8, 151.5, 153.4, 172.1. IR (KBr, cm^{-1}): 2952, 2930, 2870, 1758. Found: C, 70.07; H, 7.66; N, 6.67. Calc. for $C_{24}H_{30}N_2O_4$: C, 70.21; H, 7.38; N, 6.82%.

3,3′-Bis(dodecanoyloxy)azobenzene 3c

This was prepared in a similar way as described above in 50% yield. ^{1}H NMR ($CDCl_3$): δ(ppm) 0.88 (t, J=6.6, 6H), 1.27–1.85 (m, 36H), 2.59 (t, J=7.4, 4H), 7.19–7.84 (m, 8H). ^{13}C NMR ($CDCl_3$): δ(ppm) 14.2, 22.7, 25.0, 29.2, 29.3, 29.4, 29.5, 29.6, 32.0, 34.5, 114.9, 121.8, 124.4, 129.8, 151.5, 153.4, 172.1. Found: C, 74.52; H, 9.42; N, 4.85. Calc. for $C_{36}H_{54}N_2O_4$: C, 74.69; H, 9.42; N, 4.84%.

3,3′-Dihydroxy-2,2′-dimethylazobenzene

This was prepared by reductive coupling of 2-methyl-3-nitrophenol after protecting the hydroxy groups with 3,4-dihydro-2*H*-pyran in a way similar to that for 3,3′-dihydroxyazobenzene. In this case dry THF was used as solvent. Recrystallization from methanol–ethyl acetate (1:1) gave a dark orange solid (yield: 32% from 2-methyl-3-nitrophenol) of mp 237–238 °C. ^{1}H NMR (DMSO-d_6): δ(ppm) 2.51 (s, 6H), 6.95–7.16 (m, 6H), 9.68 (s, 2H). ^{13}C NMR (DMSO-d_6): δ(ppm) 9.8, 106.2, 116.7, 124.5, 126.2, 151.5, 156.4. IR (KBr, cm^{-1}): 3291. Found: C, 69.65; H, 5.90; N, 11.38. Calc. for $C_{14}H_{14}N_2O_2$: C, 69.39; H, 5.84; N, 11.56%.

3,3′-Bis(hexyloxy)-2,2′-dimethylazobenzene 2

This was prepared from 3,3′-dihydroxy-2,2′-dimethylazobenzene and 1-bromohexane in 77% yield. ^{1}H NMR ($CDCl_3$): δ(ppm) 0.92 (t, J=6.6, 6 H), 1.34–1.92 (m, 12 H), 2.61 (s, 6 H), 4.02 (t, J=6.3, 4 H), 6.89–7.28 (m, 6 H). ^{13}C NMR ($CDCl_3$): δ(ppm) 10.0, 14.1, 22.7, 25.9, 29.4, 31.6, 68.6, 108.2, 112.8, 126.1, 127.8, 151.9, 158.2. Found: C, 75.71; H, 9.32; N, 6.69. Calc. for $C_{26}H_{38}N_2O_2$: C, 76.03; H, 9.35; N, 6.82%.

3,3′-Bis(hexanoyloxy)-2,2′-dimethylazobenzene 4

This was prepared from 3,3′-dihydroxy-2,2′-dimethylazobenzene and hexanoyl chloride (0.47 g, 3.5 mmol) in 67% yield. ^{1}H NMR ($CDCl_3$): δ(ppm) 0.95 (t, 6 H), 1.35–1.90 (m, 12 H), 2.55 (s, 6 H), 2.64 (t, J=7.4, 4 H), 7.11–7.53 (m, 6 H). ^{13}C NMR ($CDCl_3$): δ(ppm) 10.6, 14.0, 22.4, 24.8, 31.4, 34.3, 113.6, 124.4, 126.3, 131.0, 150.4, 152.0, 172.0. IR (KBr, cm^{-1}): 2955, 2928, 2870, 1758. Found: C, 70.87; H, 8.01; N, 6.22. Calc. for $C_{26}H_{34}N_2O_4$: C, 71.19; H, 7.83; N, 6.39%.

4,4′-Dihydroxyazobenzene

Bogoslovskii's method was applied.[12] In 50 mL of distilled water was dissolved 14.2 g of $CuSO_4 \cdot 5H_2O$. Aqueous ammonia was added to the solution until a dark-blue water-soluble complex was formed. Then, aqueous $NH_2OH \cdot HCl$ was introduced to form the colorless Cu(I) complex. To this solution was added dropwise the diazonium salt of *p*-aminophenol (5.5 g, 50.5 mmol) solution prepared in advance. After stirring for 1 h, the product was extracted with ether, washed with water and dried over $MgSO_4$. The solvent was removed, and the collected solid was recrystallized from MeOH to give 1.35 g (25%) of reddish-brown solid of mp 223–224 °C. ^{1}H NMR (DMSO-d_6): δ(ppm) 6.90 (d, J=8.8, 4H), 7.70 (d, J=8.6, 4H), 10.10 (s, 2H). ^{13}C NMR (DMSO-d_6): δ(ppm) 115.8, 124.1, 145.3, 160.0. IR (KBr, cm^{-1}): 3186.

4,4′-Bis(hexyloxy)azobenzene 5

This was prepared from 4,4′-dihydroxyazobenzene and 1-bromohexane and purified by recrystallization from ethyl acetate in 67% yield. ^{1}H NMR ($CDCl_3$): δ(ppm) 0.91 (t, J=6.8, 6 H), 1.35–1.48 (m, 12 H), 1.82 (quintet, J=6.4, 4 H), 4.03 (t, J=6.5, 4 H), 6.98 (d, J=9.0, 4 H), 7.86 (d, J=9.2, 4 H). ^{13}C NMR ($CDCl_3$): δ(ppm) 14.1, 22.6, 25.7, 29.2, 31.6, 68.4, 114.7, 124.3, 147.0, 161.2. Found: C, 75.02; H, 8.89; N, 7.32. Calc. for $C_{24}H_{34}N_2O_4$: C, 75.34; H, 8.98; N, 7.32%.

4,4′-Bis(hexanoyloxy)azobenzene 6

The esterification of 4,4′-dihydroxyazobenzene with hexanoyl chloride gave an orange solid in 74% yield. ^{1}H NMR ($CDCl_3$): δ(ppm) 0.94 (t, J=7.2, 6 H), 1.38–1.86 (m, 12 H), 2.59 (t, J=7.6, 4 H), 7.24 (d, J=8.8, 4 H), 7.94 (d, J=9.0, 4 H). ^{13}C NMR ($CDCl_3$): δ(ppm) 13.9, 22.4, 24.6, 31.3, 34.4, 122.3, 124.1, 150.1, 152.9, 172.0. IR (KBr, cm^{-1}): 2953, 2930, 2870, 1748. Found: C, 70.11; H, 7.42; N, 6.86. Calc. for $C_{24}H_{30}N_2O_4$: C, 70.21; H, 7.38; N, 6.82%.

Sample preparation

Samples used in evaluating the effect of photoisomerization on LC phase stability were prepared by doping the azobenzenes at different concentrations in host LCs. Those for the nematic–isotropic equilibrium analysis were prepared by varying the concentration from 0 to 2.0 mol%. The mixtures were heated above their T_{NI} to obtain homogeneous solutions. The solutions were then injected to 5 μm thick LC cells, fabricated by glass substrates covered with a uniaxially rubbed PVA film.

Photoisomerization

E–Z Photoisomerization was performed using 350 nm light from a diffraction grating irradiator (Jasco CRM-FD) and was confirmed by tracing the electronic absorption spectra recorded on an HP8452A diode array spectrometer.

Results and discussion

Molecular design

Calamitic (rod-like) liquid crystals are usually composed of rigid core units, which are linked through a linear group or directly, with terminal chains attached to the cores so that molecular shapes should be long and narrow.[13] The *E*-isomer of azobenzene is a representative mesogen with two phenyl rings as core units that are linked through a linear -N=N- bond, and provides a range of liquid crystalline molecules through substitution with suitable terminal chains at the 4-positions. On the other hand, the *Z*-isomers of azobenzene and the related stilbenes possess a V-shaped structure and have been recognized as non-mesogenic units. In fact, the introduction of terminal substituents at both of the 4-positions of these molecules gives rise to liquid crystallinity, and this fact has given rise to a general scheme for achieving photochemical mesophase changes.[4]

Our basic idea for making the *Z*-isomers of azobenzenes compatible with LC hosts was to control the conformation of 3,3′-disubstituted azobenzenes to give the desired conformer, in which two terminal substituents at the 3,3′-positions stretch out in such a way that the molecule has a rod-like shape. 3,3′-Disubstituted azobenzenes may have three conformations for each isomer. The three conformations of *E*- and *Z*-isomers, named here as *l*- (linear), *nl*- (non-linear) and *sl*- (semi-linear) type, are shown in Fig. 2. The *l*-type is the most rod-like structure so that it should be highly compatible with LCs, whereas the *nl*-type is bent while the *sl*-type possesses an intermediate structure. Taking into account the steric hindrance due to optional substituents, it was anticipated that the introduction of small substituents at the 2- and 2′- positions would enhance the possibility of generating rod-like structures.

On the basis of the rough sketch of the molecular design, stable conformations of the isomers were optimised using CAChe (Computer Aided Chemistry) version 3.0.[14] The

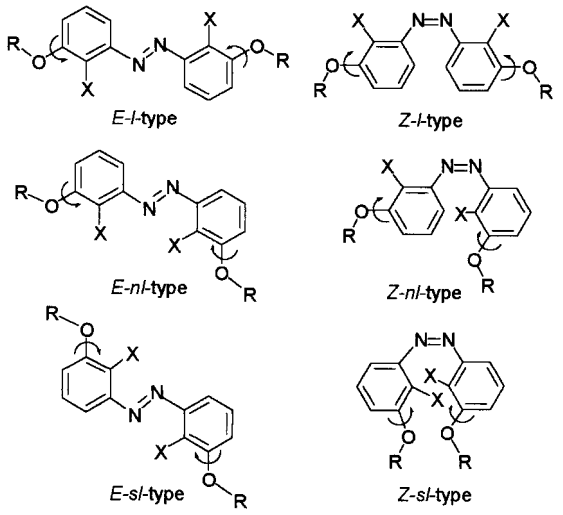

R	X	Model compound
CH_3	H	1'
CH_3	CH_3	2'
$COCH_3$	H	3'
$COCH_3$	CH_3	4'

Fig. 2 Three conformational structures of *E*- and *Z*-3,3′-disubstituted azobenzenes and the model compounds used in the Molecular Mechanics and Molecular Orbital calculation. The arrows indicate the rotation of the flexible spacers used as search parameters (dihedral angles) for optimization.

Molecular Mechanics calculations were performed using the MM2 parameter, whereas the Molecular Orbital calculations were performed with the semi-empirical MOPAC PM3 parameter. Special efforts were made in the Molecular Mechanics calculation to take into account the rotations about the two C–O bonds between the benzene rings and the spacers as shown by the arrows in Fig. 2. Four model compounds, **1**′–**4**′, were used in the calculation (see also Fig. 2). The conformations with the lowest energy calculated by MM2 were then used as initial structures for the PM3 calculation in order to obtain the optimized structures as well as the magnitudes of the heats of formation.

Synthesis and characterization of azobenzene derivatives

The synthesis of the intermediate 3,3′-dihydroxyazobenzene has already been reported by Ruggli and Hinovker,[15] who used zinc–NaOH solution as a reductive coupling agent to reduce *m*-nitrophenol. The same procedure was carried out, but it was found that the product also contained 3,3′-dihydroxyazoxybenzene. This led us to develop an alternative method using $LiAlH_4$ reduction of the aromatic nitro compounds.[16] This method was applied successfully in the synthesis of 3,3′-dihydroxyazobenzene, after first protecting the hydroxy groups of *m*-nitrophenol with 3,4-dihydro-2*H*-pyran.[17] Alkylation and esterification gave the desired azobenzenes (**1**–**4**).

The precursors to 4,4′-disubstituted azobenzenes, the 4,4′-dihydroxyazobenzenes, can be prepared by the diazo-coupling of phenol with *p*-aminophenol.[18] However, the yield was unsatisfactory (less than 10%). Instead the Bogoslovskii reaction,[12] which is a specific reaction for the preparation of *o*,*o*′-dihydroxyazo compounds, was used to prepare 4,4′-dihydroxyazobenzene in a relatively good yield and this was transformed into **5** and **6**.

The thermal analyses of the azobenzene derivatives were performed using DSC at heating and cooling rates of 2 °C per minute. The results are summarized in Table 1. It should be stressed here that some 3,3′-disubstituted azobenzenes exhibited LC phases, which were identified as the smectic phases through DSC measurement and polarizing optical microscopy. Further discussion of the LC phases of these materials will be presented elsewhere.

Table 1 Phase transition temperatures of the guests

Compounds	Phase-transition temperature/°C						
1	K	31	I				
2	K	58	S	105	I		
3a	K	96	I				
3b	K	89	I				
3c	K	97	I				
4	K	54	S	76	I		
5	K	86	S	98	N	110	I
6	K	120	S	126	I		

[a]K: crystalline, S: smectic, N: nematic, I: isotropic.

Photoisomerization characteristics

Absorption spectra of 3,3′-disubstituted azobenzenes (Fig. 3(a) and (b)) were compared to those of azobenzene and 4,4′-disubstituted azobenzenes (Fig. 3 (c)) in hexane. As can be seen, λ_{max} values for the π–π* absorptions of 3,3′-disubstituted azobenzenes and their molar extinction coefficients ε at λ_{max} are similar to those of azobenzene, whereas 4,4′-disubstituted

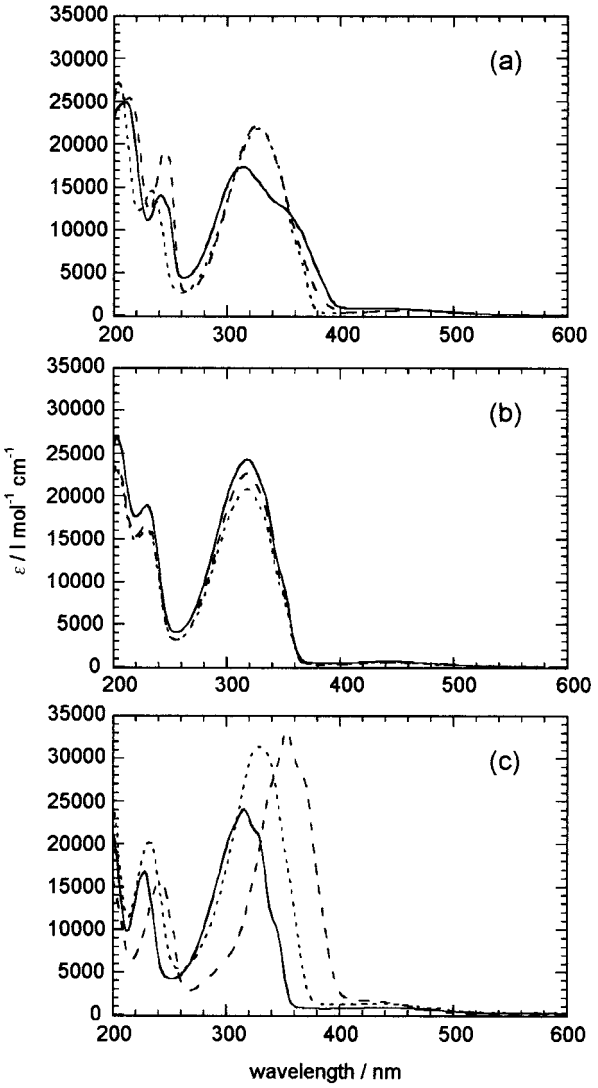

Fig. 3 Absorption spectra of *ca.* 10^{-5} M hexane solution of (a) **1** (solid line), **2** (dashed line) and **4** (dotted line); (b) **3a** (solid line), **3b** (dashed line) and **3c** (dotted line); (c) azobenzene (solid line), **5** (dashed line) and **6** (dotted line).

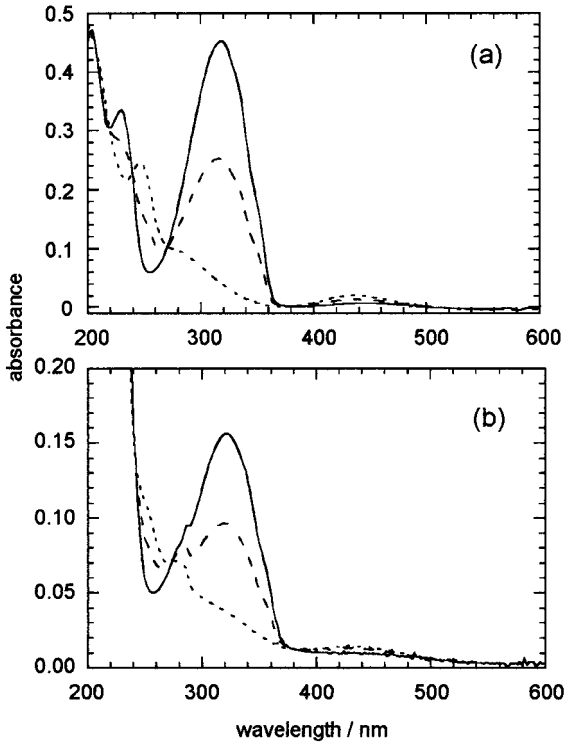

Fig. 4 Absorption spectra of **3b** during irradiation with 350 nm UV light at initial state (solid line), in the middle of reaction (dashed line), at photostationary state (dotted line), in (a) hexane solution and (b) nematic EXP-CIL within an LC cell.

azobenzenes show a larger ε with λ_{max} at a longer wavelength. *Z*-Fractions at photostationary states under illumination with 350 nm light in hexane were more than 90% for all the azobenzenes. The absorption spectral changes during photoisomerization for **3b** in hexane and in a nematic EXP-CIL are shown in Fig. 4. The photoisomerization characteristics in the nematic phase were similar to those in solutions.

Effect of photoisomerization on guest–host systems

Each guest azobenzene (concentration: 5, 10 and 20 wt%) was doped in DON-103 ($T_{NI}=73.5\,^{\circ}C$), and these binary systems were injected into empty LC cells, the inner surfaces of which were covered with a rubbed poly(vinyl alcohol) thin film to generate a homogeneous alignment. The *E–Z* photoisomerization in these highly doped systems was monitored by the n–π^* absorption changes upon irradiation with 350 nm light, as shown in Fig. 5. It was confirmed that sufficient conversion into the *Z*-isomer takes place in all cases.

In binary systems containing less than 10 wt% of azobenzene

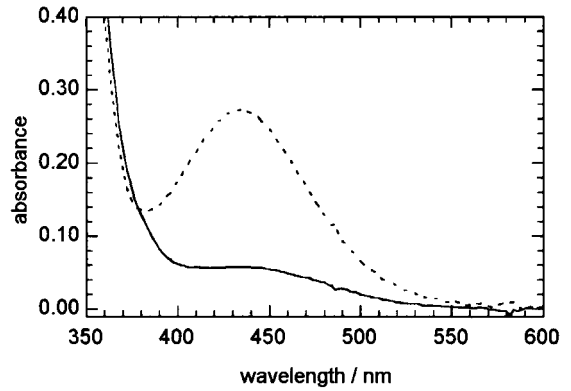

Fig. 5 Absorption spectra of *ca.* 20 wt% **3b** in DON-103 before (solid line) and after (dotted line) irradiation with UV light.

derivatives, UV light irradiation induced only a change in T_{NI} for all cases, whereas the LC phases were maintained. A distinctive effect of *Z*-isomer conformations between 3,3′-disubstituted and 4,4′-disubstituted azobenzene on LC phase stability was observed in systems loaded with 20 wt% of azobenzenes. Fig. 6 shows the photoinduced phase change of an LC system containing 20 wt% of 4,4′-disubstituted azobenzenes **5** and **6**, respectively, as a result of the formation of *Z*-isomers. Because of the solubility limitation in the higher loading, LC cells were heated at temperatures below T_{NI} of the corresponding mixtures and subjected to UV irradiation. The micrographs in this experiment were taken at the temperature where the LC phase showed the best homogeneity, which was approximately several degrees below the T_{NI} of the mixed systems. It was obvious that phase separation occurred in both systems irrespective of the nature of the *p*-substituents. Cooling the systems resulted in the appearance of crystalline domains.

Fig. 7 shows the results for the systems with 3,3′-bis(hexyloxy)azobenzene **1** and its derivative substituted with two methyl groups at the 2- and 2′-positions **2**, respectively. Unlike the systems containing **5** or **6**, which lost almost all the LC domains, these systems, although showing phase separation, still maintained large proportions of the LC domains. Although a 20 wt% loading seemed to exceed the solubility limit of the **2**–DON-103 system and resulted in crystalline domains in the homogeneous cell before light exposure, the solubility increased after UV irradiation due to *Z*-isomer formation.

Essentially, no phase change was induced photochemically when the *Z*-isomer was substituted with hexanoyloxy groups at the 3- and 3′-positions (**3b**), as shown in Fig. 8, although the preirradiation phase was not totally homogeneous due to the limited solubility. The introduction of two methyl groups at the 2- and 2′-positions displayed interesting results, as expected. The **4**–DON-103 system showed amazingly stable phase maintenance during photoisomerization, as shown in Fig. 8(c) and (d). The solubility in the LC was quite high so that homogeneous alignment without any defect was observed before UV irradiation. After UV irradiation, the homogeneous alignment was mostly maintained, suggesting that the methyl substitution at the *ortho*-position leads to the stabilization of nematic phase to a larger extent, despite the *E–Z* photoisomerization. Another interesting feature of this system is the fact that the temperature range of the nematic phase after photoisomerization was around room temperature ($T_{NI}=35.7\,^{\circ}C$ for 20 wt% doped system). These results suggested that *Z*-isomer could fit well with the host.

Nematic–isotropic equilibria of a guest–host LC

Though many studies have been carried out on the mesophase changes induced by *E–Z* photoisomerization of doped azobenzenes from an empirical standpoint to the best of our knowledge, no quantitative discussion has been made of the guest–host liquid crystal systems displaying photoinduced mesophase changes. This has led us to perform quantitative studies on photoresponsive guest–host liquid crystal systems exhibiting a photo-optical effect by means of thermodynamic measurements, in order to obtain further insight into the structure–property relationship of the systems.

With minor modifications, the Flory-Huggins theory can be adapted to describe nematic–isotropic phase equilibria.[19,20] The change of the nematic–isotropic phase transition temperature at an infinitely low guest concentration is the function of heat of transition of a nematic host and the activity coefficient of a dopant in both nematic and isotropic phases. At low concentrations of azobenzene, there exists a linear relationship between the concentration of the azobenzene guest and the change of T_{NI}, defined as reduced temperature [eqn. (1)],

$$T_{red}=T/T_0 \quad (1)$$

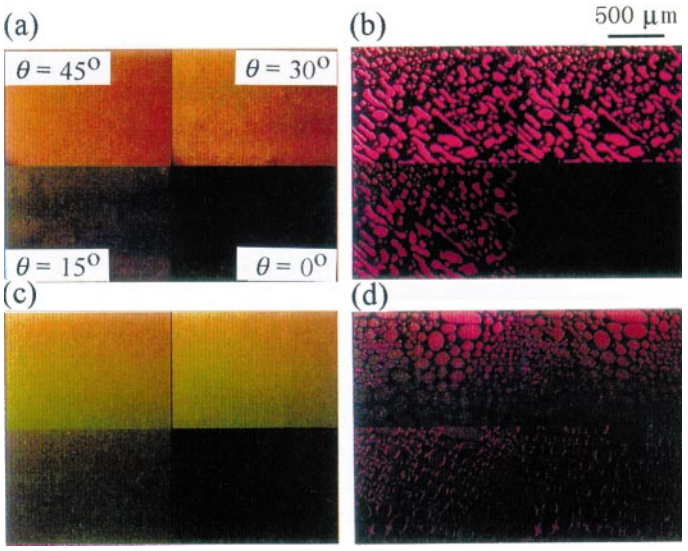

Fig. 6 Polarized micrographs of (a) **5**–DON-103 before irradiation at 75 °C, (b) after irradiation at 20 °C; and (c) **6**–DON-103 before irradiation at 75 °C, (d) after irradiation at 20 °C, with UV light. The dopant concentration is *ca.* 20 wt%. θ indicates the angle between analyzer and rubbing direction.

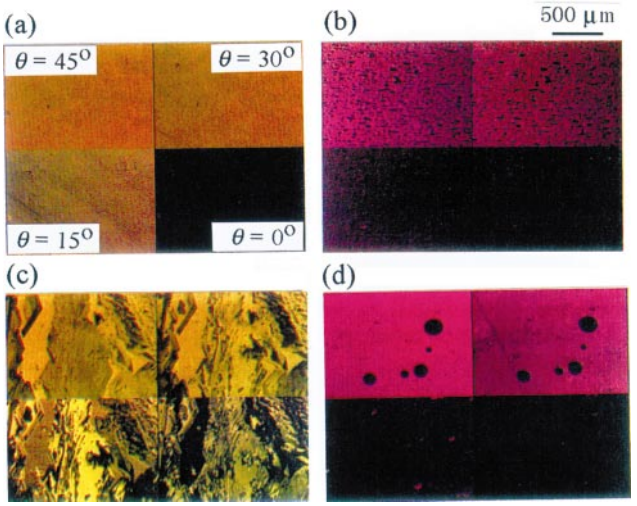

Fig. 7 Polarized micrographs of (a) **1**–DON-103 before irradiation at 20 °C, (b) after irradiation at <20 °C; and (c) **2**–DON-103 before irradiation at 57 °C, (d) after irradiation at 22 °C, with UV light. The dopant concentration is *ca.* 20 wt%. θ indicates the angle between analyzer and rubbing direction.

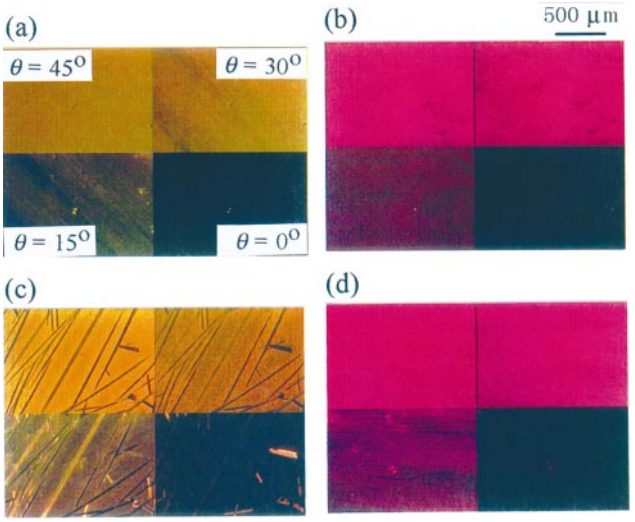

Fig. 8 Polarized micrographs of (a) **3b**–DON-103 before irradiation at 45 °C, (b) after irradiation at <20 °C; and (c) **4**–DON-103 before irradiation at 46 °C, (d) after irradiation at 30 °C, with UV light. The dopant concentration is *ca.* 20 wt%. θ indicates the angle between analyzer and rubbing direction.

where T and T_0 are T_{NI} of the guest–host LC system and of the pure nematic host, respectively. Fig. 9 shows this linear relation for the **3b**–DON-103 system. The existence of a two-phase region where the nematic and isotropic phases coexisted was confirmed in all of our systems, as first reported by de Kock.[11] The slope of the nematic–isotropic boundary, β, is a parameter connected with the compatibility of guests with the host. The higher the β value, the more compatible the guest is with the host. This fact has also been described from the viewpoint of the order parameter, S, by other workers.[10,19] Here, T^N_{red} and T^I_{red} are temperatures at which the first drop of isotropic liquid appears and the last nematic drop disappears on heating, or the last drop of isotropic liquid disappears and the first nematic drop appears on cooling, and x_g is the mole fraction of a dopant (see Fig. 9). Regardless of the difference in broadness of the two-phase areas, we derived the values of the slopes for our systems. In this case the slope β_{av} is the average value of β^N on heating and β^I on cooling. The systems were then exposed to 350 nm UV light. After confirming that the E–Z photostationary state is reached by monitoring UV

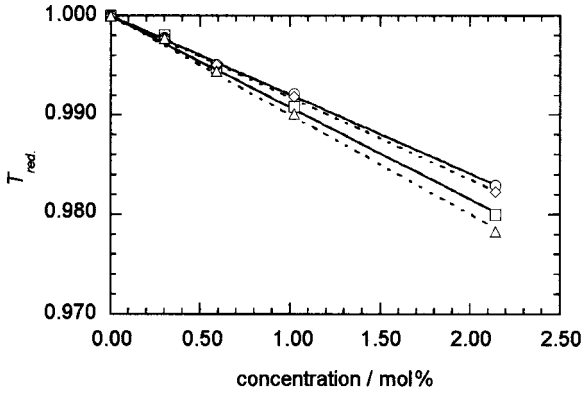

Fig. 9 The boundary of nematic–isotropic phase of **3b**–EXP-CIL system, (□) $T^N_{red.}$, (○) $T^I_{red.}$ on heating and (◇) $T^I_{red.}$, (△) $T^N_{red.}$ on cooling.

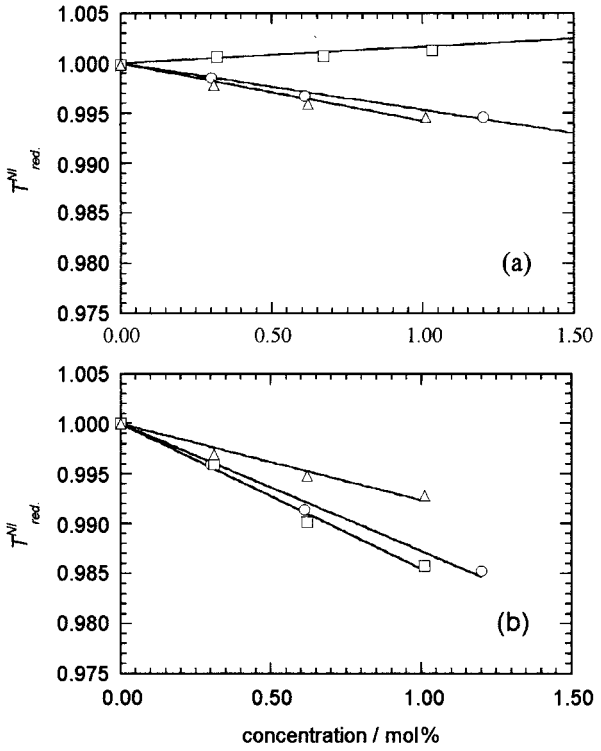

Fig. 10 Average nematic–isotropic phase boundaries of the guests (○) azobenzene, (□) **6** and (△) **4** in nematic EXP-CIL (a) before and (b) after UV light irradiation.

absorption spectra, T_{NI} was again measured. The values of the slope β_{av} before and after irradiation are shown in Fig. 10. The thermal *Z*–*E* reversion during the measurements can be ignored in the case of EXP-CIL or 5CB as host, due to their T_{NI} being close to room temperature. In the case of DON-103 as host, thermal *Z*–*E* isomerization took place during measurements because of the high T_{NI}.

To discuss guest–host compatibility in more detail, the broadness of the two-phase region and the heat of transition of the host have to be considered. Therefore, the transformation of thermodynamic properties to those of the infinitely dilute solution, which was described by Kronberg *et al.*,[19] is necessary. The transformation formulas are given in eqn. (2) and (3):

$$\beta^{N\infty} = \frac{\beta^{N}}{\left(1+\frac{\kappa-\kappa^{\infty}}{(\beta^{N})^{-1}+(\beta^{I})^{-1}}\right)} \quad (2)$$

$$\beta^{I\infty} = \frac{\beta^{I}}{\left(1-\frac{\kappa-\kappa^{\infty}}{(\beta^{N})^{-1}+(\beta^{I})^{-1}}\right)} \quad (3)$$

where, $\kappa=(\beta^{N})^{-1}-(\beta^{I})^{-1}$, and $\kappa^{\infty}=\Delta H_0/RT_0$. ΔH_0 is the heat of nematic–isotropic transition of the pure host. ΔH_0 values for nematic EXP-CIL, 5CB and DON-103 are 956.34, 748.20 and 978.24 J mol^{-1}, respectively. Another useful parameter $r_2\Delta\chi$ is related to activity coefficients of the guest γ_g and β through eqn. (4)

$$\ln(\beta^{N\infty}/\beta^{I\infty}) = \ln({\gamma_g}^{N\infty}/{\gamma_g}^{I\infty}) = r_g\Delta\chi \quad (4)$$

$r_g\Delta\chi$ corresponds to the *interchange free energy parameter* of the guest and host. The thermodynamic data are listed in Table 2. As can be seen from the Table, 4,4′-disubstituted azobenzene–EXP-CIL systems (runs 2 and 3) enhanced the stability of the system strongly, being indicated by small values of $r_g\Delta\chi$. However, when photoisomerized, a large increase in the value was observed. This can be understood by considering the conformational change from the *E*- to *Z*-form which induces the disordering of the system and may lead to phase separation as already shown above. The difference in $r_g\Delta\chi$ for

Table 2 Thermodynamic data of guest–host nematic LC systems before and after UV light irradiation

			Before UV light irradiation				
Run	Guest	Host	β^{N}	β^{I}	$\beta^{N\infty}$	$\beta^{I\infty}$	$r_g\Delta\chi$
1	Azobenzene	EXP-CIL	−0.46	−0.42	−0.48	−0.40	0.17
2	**5**	EXP-CIL	0.23	0.29	0.25	0.27	−0.10
3	**6**	EXP-CIL	0.16	0.20	0.18	0.19	−0.07
4	**1**	EXP-CIL	−0.90	−0.77	−0.98	−0.71	0.31
5	**2**	EXP-CIL	−0.58	−0.45	−0.56	−0.47	0.19
6	**3a**	EXP-CIL	−0.93	−0.75	−0.98	−0.71	0.31
7	**3b**	EXP-CIL	−0.94	−0.80	−1.03	−0.74	0.33
8	**3c**	EXP-CIL	−1.05	−0.83	−1.11	−0.78	0.35
9	**3b***[a]	EXP-CIL	—	—	—	—	—
10	**4**	EXP-CIL	−0.60	−0.51	−0.62	−0.50	0.21
11	**4**	5CB	−0.66	−0.59	−0.69	−0.53	0.27
12	**4**	DON-103	−0.43	−0.37	−0.43	−0.37	0.15
			After UV light irradiation				
Run	Guest	Host	β^{N}	β^{I}	$\beta^{N\infty}$	$\beta^{I\infty}$	$r_g\Delta\chi$
1	Azobenzene	EXP-CIL	−1.41	−1.14	−1.63	−1.01	0.48
2	**5**	EXP-CIL	−1.44	−1.09	−1.60	−1.00	0.47
3	**6**	EXP-CIL	−1.62	−1.23	−1.85	−1.09	0.53
4	**1**	EXP-CIL	−1.18	−0.97	−1.31	−0.88	0.40
5	**2**	EXP-CIL	−1.32	−0.96	−1.40	−0.91	0.42
6	**3a**	EXP-CIL	−1.13	−0.89	−1.21	−0.83	0.38
7	**3b**	EXP-CIL	−1.26	−0.99	−1.38	−0.91	0.42
8	**3c**	EXP-CIL	−1.26	−0.83	−1.24	−0.84	0.38
9	**3b***[a]	EXP-CIL	−1.21	−1.00	−1.36	−0.90	0.41
10	**4**	EXP-CIL	−0.85	−0.69	−0.88	−0.66	0.29
11	**4**	5CB	−0.83	−0.70	−0.85	−0.58	0.39
12	**4**[b]	DON-103	−0.65	−0.56	−0.67	−0.53	0.23

[a]Pure *Z*-isomer of **3b** separated by column chromatography. [b]The data after irradiation involved approximately 10% of thermal *Z*–*E* isomerization.

these systems was very high (more than 0.5) compared to other systems.

Let us now compare **3a**, **3b**, and **3c**–EXP-CIL systems (runs 6, 7 and 8) which are different only in the length of the flexible chains. In their *E*-forms, extending the chain slightly increased the $r_g\Delta\chi$. However, such a relationship was not observed after irradiation. It is proper to assume that in the range of these alkyl sizes, the difference of the chain length is not an essential factor influencing the $r_g\Delta\chi$. For a non-mesomorphic solute–nematic system, the independence of *n*-alkane size and the order parameter has been described.[18] The same conclusion seems to be appropriate also for our mesomorphic solute–nematic systems. After UV irradiation, these samples possess smaller values of $r_g\Delta\chi$ compared to **5** or **6**–EXP-CIL systems. The difference from those before UV irradiation was less than 0.1. The same result was also confirmed for the **4**–EXP-CIL system (run 10), in which methyl groups are attached to the 2- and 2′-positions of the azobenzene core. This suggests that the *Z*-conformers are nearly as compatible with the host as the *E*-conformers. In fact, **4**-containing systems show the smallest $r_g\Delta\chi$ among those with the 3,3′-disubstituted azobenzenes, which support our prediction of the effectiveness of steric hindrance caused by a methyl group to the stability of the rod-like *Z*-structure.

In the case of the system containing 3,3′-disubstituted azobenzene with ether groups, **1** (run 4), the change of $r_g\Delta\chi$ was no larger than for those with ester groups, **3** or **4**, while that for **2** (run 5) was somewhat larger but still smaller than those for 4,4′-disubstituted azobenzenes, **5** and **6**. These intermediate values may be the reason for the slight photo-induced phase separation as demonstrated above. This behavior will be explained later by comparison with the theoretically stable *Z*-conformers of the corresponding guests.

Another comparison was made for **3b** and **3b***–EXP-CIL systems (runs 7 and 9) where **3b*** is a pure *Z*-isomer of **3b**, which was isolated and purified by column chromatography on silica gel. The two systems were identical in all features, implying that the *E*–*Z* photoisomerization proceeds to a great extent in the LC host.

The effect of the host was examined by comparing systems containing **4** (runs 10, 11 and 12). Obviously, hosts with higher nematic–isotropic transition enthalpy ΔH_0 (DON-103 > EXP-CIL > 5CB) are much more stable because of the high nematic phase ordering. However, in order to suppress the thermal *Z*–*E* reverse isomerization, hosts with relatively low T_{NI} were preferable in the experiments. The features in the **4**–DON-103 system (run 12) involved approximately 10% of this effect as monitored by UV absorption spectra after T_{NI} measurement.

Correlation between calculated and experimental data

Rod-like structures of molecules are essential in creating a calamitic LC phase, which can be induced by introducing flexible substituents to the ends of a mesogenic unit. In the case of photoresponsive azobenzenes, extending the 4,4′-position is a well-known method in creating liquid crystalline substances, but the formation of its bent *Z*-isomers will destroy the LC phase to a certain extent. We have performed molecular orbital calculations and shown that LC systems with a new type of dopants, the 3,3′-disubstituted azobenzenes, can exhibit phase stability upon *E*–*Z* isomerization. Good correlation was obtained between calculated and experimental results, as mentioned above. The dihedral angles and the heat of formation were calculated with the procedure described above, and the results are summarized in Table 3. The signs of the dihedral angles indicate the relative rotational position between the two planes, positive being clockwise and negative being anti-clockwise rotation.

In the model compound, **1**′, there were no significant differences in the heat of formation between *l*-, *nl*- and *sl*-type conformations in either the *E*- or *Z*-isomer. In the *E*-isomer of **3**′, the differences seem to be more pronounced. The *E-l*- and *E-nl*-type were likely to be more stable than the *E-sl*-type. The same tendency was also observed among the *Z*-confor-

Table 3 Dihedral angles and heat of formation, calculated by PM3 for the four model compounds

Model compound	Dihedral angles (°)					Heat of formation/ kcal mol^{-1}
	C(1)-N=N-C(1′)	C(4)-C(3)-O-C	C(4′)-C(3′)-O-C′	N=N-C(1)-C(2)	N=N-C(1′)-C(2′)	
1′						
E-l type	−180.0	−1.0	−2.5	−169.8	171.0	15.99
E-nl type	−178.9	1.4	177.7	0.8	179.0	15.80
E-sl type	−180.0	−0.9	−0.6	3.9	−3.4	15.79
Z-l type	−5.6	−4.0	−2.7	141.3	139	19.29
Z-nl type	−3.7	−4.6	179.7	135.9	−44.2	18.92
Z-sl type	0	176.6	179.7	51.3	45.8	18.51
2′						
E-l type	−177.0	−2.2	−6.7	−157.0	156.2	6.30
E-nl type	−178.9	2.6	9.9	−167.0	−14.0	7.87
E-sl type	179.6	0	8.9	34.4	−32.3	9.34
E-l type	−4.0	−8.8	0.3	139.5	136.9	8.47
Z-nl type	−1.7	−2.7	6.8	136.6	−61.4	9.12
Z-sl type	6.8	−92.3	0.9	−56.6	−55.0	11.77
3′						
E-l type	175.4	−109.3	48.7	−171.7	164.9	−69.62
E-nl type	−176.0	−161.3	−50.6	31.0	149.8	−67.55
E-sl type	176.8	−51.0	26.6	21.5	−18.0	−68.04
E-l type	4.6	−15.9	28.3	−141.3	−137.8	−63.50
Z-nl type	0.4	138.2	10.7	48.4	−135.5	−64.94
Z-sl type	2.3	−150.4	−146.2	−43.0	−45.0	−62.94
4′						
E-l type	180.0	−49.5	48.3	−169.2	170.0	−78.30
E-nl type	177.3	38.8	43.4	140.6	45.8	−76.67
E-sl type	−177.6	60.3	48.4	−24.9	28.0	−75.29
E-l type	0.9	59.7	64.8	−134.5	−138.4	−78.37
Z-nl type	0.9	45.3	40.9	134.0	61.2	−74.81
Z-sl type	−5.7	42.9	49.4	57.8	57.9	−73.45

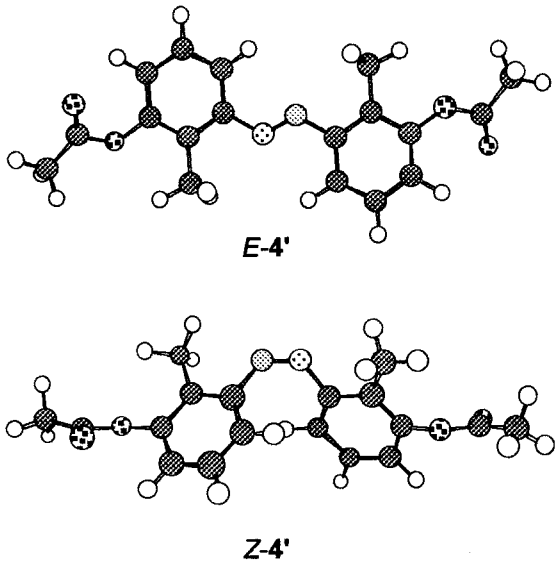

Fig. 11 Structures of *E*-**4**′ and *Z*-**4**′.

mers. Comparing these two model compounds, it is reasonable to say that **3**′ was more likely to adopt a rod-like structure (the *l*-type isomers), although some portion of non-rod-like structures might coexist due to the small energy differences. The non-rod-like structures can possibly be suppressed to some extent when this compound is in an LC environment, because of the interaction with the rod-like LC molecules. This is in agreement with the experimental results for **3** containing systems (Fig. 8 (a), (b) and run 7 in Table 2).

In accord with our expectations, the rod-like-generating effect is intensely pronounced when relatively small substituents such as methyl are attached to the 2- and 2′-positions of the 3,3′-disubstituted azobenzene. In model compounds, **2**′ without the dimethyl and **4**′ with dimethyl groups, it is obvious that the *E-l*-types of both compounds are preferred. The *Z-l*- and *Z-nl*-types of **2**′ may exist as relatively stable conformers since the energy difference is somewhat small. However, the *Z-l*-type of **4**′ was undoubtedly the most stable one among the conformers of this compound, as indicated by the significant difference in the heat of formation. This is also supported by the fact that the *E-l*-type and *Z-l*-type of **4**′ exhibit equal values of heat of formation. Notice also that these two isomers have elongated rod-like structures as shown in Fig. 11. The fact that $r_g\Delta\chi$ of the **4**–EXP-CIL system after irradiation is much smaller than that of the **2**–EXP-CIL system is due to the relatively large difference in the energy between its *Z-l*-type and *Z-nl*- or *Z-sl*-type conformers. The difference in the phase stability for these two systems, as shown qualitatively in Fig. 7 and 8, can also be explained by means of the difference in the heat of formation. It is worth noticing also that the optimized structures provide the information that the dipole moments of substituents orient in such a position that the total dipole moments are minimised. This may be the reason that the compound with the ester groups is more rod-like than that with the ether groups.

Conclusion

The molecular design and synthesis of novel type photoresponsive dopants, 3,3′-disubstituted azobenzenes, were performed with the aim of developing a photoresponsive nematic LC system that exhibits phase stability during photoisomerization. We discovered that appropriate substituents realize our objective. The guests, **3** and **4**, are the best candidates since they, in both *E*- and *Z*-conformers, exhibit the lowest interchange free energy in the host LC, and thus maintain the phase stability of the system, which is not observable in the case of 4,4′-disubstituted azobenzenes.

Stable *E*- and *Z*-conformations of each guest were calculated by Molecular Mechanics and Molecular Orbital methods. The calculated molecular structures and their heats of formation were compared to the thermodynamic properties of experimental data to reveal a reasonable correlation between them. The results also suggested that substituent dipoles and steric hindrance play an important role in controlling the conformation of the novel azobenzenes.

References

1 M. W. Gibbons, T. Kosa, P. P. Murohay and P. J. Shannon, *Nature*, 1995, **377**, 43.
2 T. Sasaki, T. Ikeda and K. Ichimura, *Macromolecules*, 1992, **25**, 3807.
3 R. H. Berg, S. Hvilsted and P. S. Ramanujam, *Nature*, 1996, **383**, 505.
4 K. Ichimura, in *Photochromism; Molecules and Systems*, ed. H. Dürr and H. Bouas-Laurent, Elsevier, Amsterdam, 1990, p. 903.
5 W. W. Haas, K. F. Nelson, J. E. Adams and G. A. Dir, *J. Electrochem. Soc.*, 1974, **121**, 1667.
6 S. Tazuke, S. Kurihara and T. Ikeda, *Chem. Lett.*, 1987, 911.
7 E. Sackmann, *J. Am. Chem. Soc.*, 1971, **93**, 7088.
8 G. Heppke, H. Marschall, P. Nurnberg, F. Oestreicher and G. Scherowsky, *Chem. Ber.*, 1981, **114**, 2501.
9 D. S. Hermann, P. Rudquist, K. Ichimura, K. Kudo, L. Komitov and S. T. Lagerwall, *Phys. Rev. E*, 1997, **55**, 2857.
10 D. Bauman, *Mol. Cryst. Liq. Cryst.*, 1988, **159**, 197.
11 A. C. de Kock, *Z. Phys. Chem.*, 1904, **48**, 129.
12 B. M. Bogoslovskii, *J. Gen. Chem. USSR*, 1946, **16**, 193.
13 P. J. Collings and M. Hird, in *Introduction to Liquid Crystals; Chemistry and Physics*, Taylor and Francis, London, 1997.
14 *Cache Reference*, ver. 3.0, CaChe Scientific Inc., USA, 1992.
15 P. Ruggli and M. Hinovker, *Helv. Chim. Acta*, 1934, **17**, 411.
16 R. F. Nystrom and W. G. Brown, *J. Am. Chem. Soc.*, 1948, **70**, 3738.
17 N. Grant, V. Perlog and R. P. A. Sneedan, *Helv. Chim. Acta*, 1963, **46**, 415.
18 S. R. Sandler and W. Karo, in *Organic Functional Group Preparations*, 2nd edn., Academic Press Inc., 1986, ch. 14.
19 B. Kronberg and D. Patterson, *J. Chem. Soc., Faraday Trans. II*, 1976, **72**, 1687; B. Kronberg, D. F. R. Gilson and D. Patterson, *J. Chem. Soc., Faraday Trans. II*, 1976, **72**, 1673.
20 G. R. Luckhurst and G. W. Gray, in *The Molecular Physics of Liquid Crystals*, Academic Press, London, 1979, ch. 10 and 11.

Paper 8/08083F